Available online at www.sciencedirect.com
SCIENCE DIRECT
Journal of Molecular Catalysis A: Chemical 250 (2006) 122–130
JOURNAL OF MOLECULAR CATALYSIS A: CHEMICAL
www.elsevier.com/locate/molcata

Selective oxidation of methane to formaldehyde over antimony oxide-loaded catalyst

Hiroyuki Matsumura [a], Kimito Okumura [a], Takahiro Shimamura [a], Na-oki Ikenaga [a], Takanori Miyake [a,b], Toshimitsu Suzuki [a,b,*]

[a] *Department of Chemical Engineering, Kansai University, Suita, Osaka 564-8680, Japan*
[b] *High Technology Research Center, Kansai University, Suita, Osaka 564-8680, Japan*

Received 8 June 2005; received in revised form 23 January 2006; accepted 24 January 2006
Available online 28 February 2006

Abstract

A possibility of antimony oxide as a catalyst for the selective oxidation of methane with oxygen to formaldehyde was investigated. The activity measurement was carried out at an atmospheric pressure and at 873 K, where the homogeneous gas-phase reaction was negligible. Oxidized diamond (O-Dia)-supported antimony oxide catalyst produced 1.3 mmol h^{-1} g-cat^{-1} of formaldehyde with a formaldehyde selectivity of 23%. On the other hand, SiO_2 supported antimony oxide catalyst exhibited negligible catalytic activity. XRD and UV–vis analyses revealed that α-Sb_2O_4 was formed on the oxidized diamond while Sb_6O_{13} was formed on SiO_2. Selective oxidation of methane to formaldehyde seemed to proceed on α-Sb_2O_4 with moderate activity and selectivity to formaldehyde, via a redox cycle of α-Sb_2O_4 and Sb_2O_{4-x}. On the other hand, Sb_6O_{13} on SiO_2 was stable under the reaction conditions and the selective oxidation occurred only slightly.

Keywords: Oxidation; Methane; Formaldehyde; Oxidized diamond; XRD; Redox cycle

1. Introduction

Formaldehyde is widely used as a raw material for resins and adhesives, and is industrially produced in a three-step process. Therefore, direct conversion of methane with oxygen to formaldehyde is one of the most challenging chemistry in the field of catalytic science.

Selective oxidation of methane to formaldehyde has been carried out with supported transition metal oxides, particularly molybdenum oxide [1–8], iron oxide [9,10] and vanadium oxides [1,2,11–14]. Vanadium oxide on MCM-41or -48 [15] and vanadium and iron oxides on MCM-41 were reported to exhibit high performance [16].

Tabata et al. reported that addition of NO_x as an oxidant promoted the selective oxidation of methane to formaldehyde and methanol with MoO_3 and MoO_3/SiO_2 catalysts [17–19].

Although a large number of catalysts have been reported, none of them has satisfied the requirements for commercialization. Since the oxidation of methane requires a high reaction temperature to activate relatively inert methane on catalysts, deep oxidations of primary products to give CO_x occur more easily than the formation of oxygenates because of the weaker C–H bond in formaldehyde than that in methane [20]

$$CH_4 + O_2 \rightarrow HCHO + H_2O, \quad \Delta H^\circ_{298} = -319\,\text{kJ/mol} \qquad (1)$$

$$HCHO + O_2 \rightarrow CO_2 + H_2O, \quad \Delta H^\circ_{298} = -571\,\text{kJ/mol} \qquad (2)$$

We have recently reported that oxidized diamond (O-Dia)-supported catalysts exhibit high catalytic performance in various reactions [21–23]. The surface of O-Dia is considered as a pseudo-solid carbon oxide phase which does not exist above ambient temperature.

Ni- and Co-loaded O-Dia catalysts showed significant catalytic activity in the partial oxidation of methane to the synthesis gas [22]

$$CH_4 + 1/2O_2 \rightarrow CO + 2H_2, \quad \Delta H^\circ_{298} = -36\,\text{kJ/mol} \qquad (3)$$

Furthermore, we have first reported that V_2O_5-loaded O-Dia catalyst produced formaldehyde and acetaldehyde from methane

* Corresponding author. Fax: +81 6 6388 8869.
E-mail address: tsuzuki@ipcku.kansai-u.ac.jp (T. Suzuki).

1381-1169/$ – see front matter © 2006 Elsevier B.V. All rights reserved.
doi:10.1016/j.molcata.2006.01.043

and ethane with CO_2 as a mild oxidant [23–25]

$$CH_4 + 2CO_2 \rightarrow HCHO + 2CO + H_2O,$$
$$\Delta H^{\circ}_{298} = +246\,kJ/mol \quad (4)$$

$$C_2H_6 + 2CO_2 \rightarrow CH_3CHO + 2CO + H_2O,$$
$$\Delta H^{\circ}_{298} = +195\,kJ/mol \quad (5)$$

In these reactions, weak adsorption of produced oxygenates on the catalyst surface decreased chances of deep oxidation of the products.

Antimony oxides are widely used as a key promoter in mixed oxide catalysts for the ammoxidation of propane to acrylonitrile [26–36] and the partial oxidation of propane or propene to acrylic acid [37–41]. Antimony oxides are considered to promote the rate-limiting abstraction of hydrogen from hydrocarbon molecules, as well as the subsequent oxygen insertion into allylic intermediate species [38]. However, only one paper dealt with the antimony oxide single phase catalyst in the oxidation of methane to formaldehyde [42]. Methane conversion of 0.4–1.0% with formaldehyde selectivity less than 30% was obtained at a low space velocity.

This paper deals with antimony oxide based catalysts for the selective oxidation of methane to formaldehyde. We have found that antimony oxide loaded on O-Dia exhibited moderate catalytic activity for the oxidation of methane to formaldehyde with a reasonable selectivity.

2. Experimental

2.1. Materials

As support materials, powdered diamond (General Electric Co., surface area (SA) = 23 m^2/g), SiO_2 (Fuji Silicia Chem. Co., SA = 110, 208 m^2/g, and Fuso Chemicals, SA = 12 m^2/g), GeO_2 (Kishida Chemicals, SA < 1 m^2/g), Al_2O_3 (Sumitomo Chemical Ind., SA = 159 m^2/g), MgO (Ube Materials Ind., SA = 144 m^2/g), TiO_2 (Japan aerosil, SA = 50 m^2/g) and ZrO_2 (prepared by themal decomposition of $Zr(OH)_4$, SA = 46 m^2/g) were used. Antimonic acid (H_3SbO_4) was used as the antimony oxide source. Commercial $SbCl_5$, Sb_2O_5, Sb_2O_4 and Sb_2O_3 were purchased from Wako Chemicals.

2.1.1. Preparation of antimonic acid

Antimonic acid was prepared by dropwise addition of $SbCl_5$ to a 30% aqueous solution of H_2O_2 at 273 K. The white precipitate of antimonic acid was filtered off after ageing for 6 h at 273 K, washed three times with distilled water and then dried at 383 K overnight.

2.1.2. Preparation of oxidized diamond

Man-made industrial diamond of fine particles less than 0.5 μm in diameter was hydrogenated at 1173 K for 1 h under pure H_2 stream. The hydrogenated diamond was partially oxidized at 723 K for 5 h under air stream. Thus obtained O-Dia is known to have functional groups of C–O–C and C=O on the carbon surface [24,25,43].

2.1.3. Preparation of catalysts

All the catalysts were prepared by a usual impregnation method. Antimony oxide-loaded O-Dia catalysts were prepared by impregnating O-Dia powder with an aqueous solution of antimonic acid and oxalic acid. The suspension was kept stirring and refluxing for 3 h, followed by stirring at room temperature for 24 h. Excess water was removed under vacuum, and the obtained catalyst precursor was calcined at 723 K for 3 h in the presence of air.

The loading level of antimony oxide onto supports is expressed by weight percentages of oxides; wt.% = (weight of metal oxide)/(weight of metal oxide and support) × 100.

2.2. Activity measurement

A fixed-bed flow type reactor (quartz, i.d. 10 mm) was used for measurement of the catalyst performance at an atmospheric pressure. A 100 mg of catalyst was placed in the center of the reactor tube with quartz wool plugs. A reaction gas mixture consistings of CH_4 and O_2 was passed through the catalyst bed a flow rate of 30 mL/min at an atmospheric pressure (space velocity = 18,000 mL h^{-1} g-cat^{-1}). Oxygenates were analyzed by an on-line high speed gas chromatograph (Chrompack CP-2002, GL Science Corp.) using a thermal conductivity detector with CP CIL 5CB and HYESEP A columns. CO and CO_2 were analyzed by a Shimadzu GC8AIT gas chromatograph, equipped with a TCD detector using an activated carbon column (3 mm × 2 m).

2.3. Characterization

UV–vis absorption spectra of the catalysts were obtained with a diffuse reflectance mode by diluting the catalyst with SiO_2 using a Jasco model V-550.

X-ray diffraction (XRD) measurements were performed with a Shimadzu XRD-6000 with monochromatized Cu Kα radiation. X-ray photoelectron spectra were obtained with a Jeol model JPS900 using Mg Kα radiation.

3. Results and discussion

3.1. Effect of metal oxides on the selective oxidation of methane to formaldehyde

Table 1 shows the effect of metal oxides on the selective oxidation of methane to formaldehyde. Although V_2O_5- and Bi_2O_3-loaded O-Dia catalysts produced large amounts of CO_x (runs 2, 4), MoO_3- and antimony oxide- loaded O-Dia catalysts afforded considerable amounts of formaldehyde (runs 1, 3). In particular, antimony oxide-loaded O-Dia catalyst gave a large amount of formaldehyde with a moderate selectivity.

3.2. Effect of various supports on the selective oxidation of methane to formaldehyde

Since antimony oxide afforded the highest HCHO yield among the oxides tested, the effect of various supports on the selective oxidation of methane was examined. The results are

Table 1
Effect of loading metal on the selective oxidation of methane

Run	Loading metal	Conv. (%)	Yield (mmol h^{-1} g-cat^{-1})			Selectivity (%)		
			HCHO	CO	CO_2	HCHO	CO	CO_2
1	Sb oxide	0.88	1.31	2.59	1.61	23.9	47.0	29.2
2	V_2O_5	7.91	0.16	18.8	37.7	0.3	33.1	66.6
3	MoO_3	0.84	0.36	2.61	2.15	7.1	51.0	41.9
4	Bi_2O_3	2.65	0.05	0.36	15.8	0.3	2.2	97.5

Catalyst: 100 mg, loading loading: 3 wt.%, reaction temperature: 873 K, gas flow: 30 mL/min (CH_4/O_2 = 25/5), SV: 18,000 mL h^{-1} g-cat^{-1}, reaction time: 90 min.

shown in Table 2. Group 14 oxides, SiO_2 and GeO_2, are selected to compare with O-Dia, and Al_2O_3, MgO, TiO_2 and ZrO_2 are selected as typical catalyst supports. As is shown, O-Dia supported catalyst exhibited the highest catalytic activity in the selective oxidation of methane to formaldehyde among the support materials examined (run 5). SiO_2 and GeO_2 supported catalysts afforded low activity (runs 6, 9), and Al_2O_3, MgO, TiO_2 and ZrO_2 supported catalysts produced large amounts of CO_x (runs 10–13). High surface area SiO_2 was employed as supports in order to see the effect of surface area on the catalytic performance of loaded SbO_x. However, as seen in runs 7 and 8 in Table 2, no increases in HCHO yields were observed for the high surface area SiO_2

$$CH_4 + 2O_2 \rightarrow CO_2 + 2H_2O, \quad \Delta H^\circ_{298} = -801\,\text{kJ/mol} \tag{6}$$

$$HCHO \rightarrow CO + H_2, \quad \Delta H^\circ_{298} = -1.87\,\text{kJ/mol} \tag{7}$$

$$HCHO + O_2 \rightarrow CO_2 + H_2O, \quad \Delta H^\circ_{298} = -571\,\text{kJ/mol} \tag{8}$$

Basic supports, MgO and ZrO_2, did not give even a trace amount of formaldehyde (runs 12, 13). These results seem to indicate that a support having weak interaction with antimony oxide afforded a high activity for the selective oxidation of methane.

3.3. Effect of various supports on the selective oxidation of ethane to oxygenates

Table 3 shows the effect of various supports on the selective oxidation of ethane to oxygenates. The activity order of the antimony oxide-loaded support materials was similar to what was observed with methane. However, ethane conversions were slightly higher than those of methane, since dehydrogenation of ethane to ethylene proceeded to some extent

$$C_2H_6 + 1/2O_2 \rightarrow C_2H_4 + H_2O, \quad \Delta H^\circ_{298} = -148\,\text{kJ/mol} \tag{9}$$

O-Dia supported catalyst produced a considerable amount of formaldehyde instead of the expected product, acetaldehyde (run 14). To study a possibility of decomposition of acetaldehyde to formaldehyde, the reaction of acetaldehyde was examined. The results are shown in Fig. 1. Without catalyst, acetaldehyde decomposed to formaldehyde, CO and CO_2 (Fig. 1a). O-Dia supported catalyst exhibited a higher acetaldehyde conversion than the thermal reaction without catalyst at all the reaction temperatures. In the thermal reaction, the formaldehyde selectivity decreased with increasing reaction temperature, indicating that formaldehyde is decomposed to CO at a high reaction temperature.

In the selective oxidation of lower alkanes to oxygenates, a key step seems to be desorption of produced oxygenates from the catalyst surface. When the desorption of oxygenates from the catalyst is slow, the oxygenates tend to decompose to CO_x. Since the O-Dia supported catalyst showed a moderate formaldehyde selectivity even at a high reaction temperature, desorption of formaldehyde from the catalyst surface would be rapid. Thus, O-Dia supported catalyst could produce formaldehyde without excessive decomposition into CO_x [23]

$$CH_3CHO \rightarrow HCHO \rightarrow CO, CO_2 \tag{10}$$

Table 2
Effect of various supports on the selective oxidation of methane

Run	Support	Conv. (%)	Yield (mmol h^{-1} g-cat^{-1})			Selectivity (%)		
			HCHO	CO	CO_2	HCHO	CO	CO_2
5	O-Dia	0.88	1.31	2.59	1.61	23.9	47.0	29.2
6	SiO_2	0.13	0.46	0.06	0.26	58.8	7.3	34.0
7	SiO_2[a]	0.08	0.45	0.03	0.04	89.1	5.3	5.6
8	SiO_2[b]	0.11	0.29	0.16	0.17	47.5	25.5	27.0
9	GeO_2	0.06	0.33	0	0	100.0	0	0
10	Al_2O_3	1.67	0.24	6.61	3.98	2.2	61.1	36.8
11	MgO	1.87	0	2.68	5.19	0	34.0	66.0
12	TiO_2	0.49	0.15	1.46	1.20	5.4	51.9	42.7
13	ZrO_2	2.72	0	0.69	15.2	0	4.4	95.6

Catalyst: 100 mg, Sb_2O_4 loading: 3 wt.%, reaction temperature: 873 K, gas flow: 30 mL/min (CH_4/O_2 = 25/5), SV: 18,000 mL h^{-1} g-cat^{-1}, reaction time: 90 min.
[a] Surface area 101 m^2/g.
[b] Surface area 490 m^2/g.

Table 3
Effect of various supports on the selective oxidation of ethane

Run	Support	Conv. (%)	Yield (mmol h^{-1} g-cat^{-1})						Selectivity (%)	
			HCHO	CH_3CHO	CH_4	C_2H_4	CO	CO_2	HCHO	CH_3CHO
14	O-Dia	0.95	1.89	0.33	0.12	2.16	2.22	1.72	17.3	6.1
15	SiO_2	0.51	0.07	0.06	0.03	2.73	0.06	0.05	1.2	2.0
16	GeO_2	0.60	0.06	0.11	0	3.22	0.02	0	0.9	3.1
17	Al_2O_3	2.62	0.05	0.50	0.28	3.36	9.97	11.5	0.2	1.4
18	MgO	2.26	0	0.07	0.35	2.66	5.15	15.8	0	0.6

Catalyst: 100 mg, Sb_2O_4 loading level: 3 wt.%, reaction temperature: 823 K, gas flow: 30 mL/min ($C_2H_6/O_2 = 25/5$), SV: 18,000 mL h^{-1} g-cat^{-1}, reaction time: 90 min.

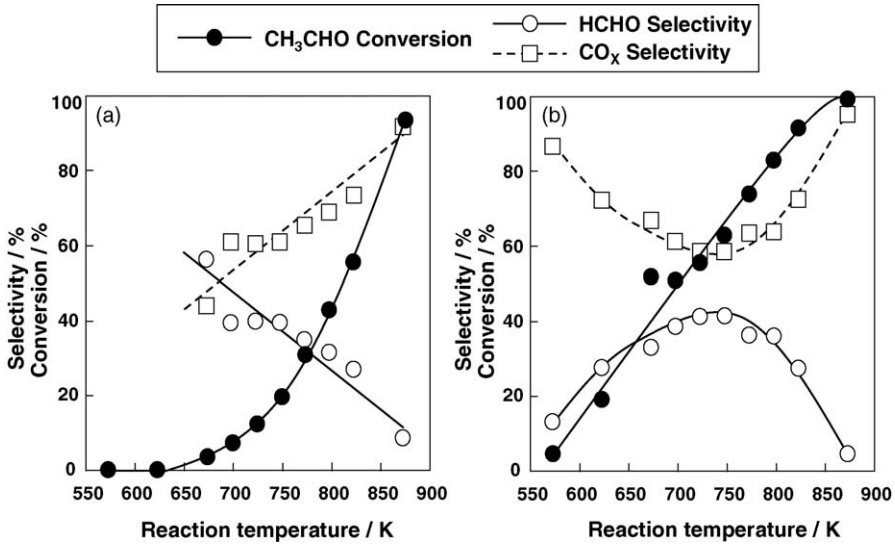

Fig. 1. Effect of reaction temperature on the decomposition of acetaldehyde (a) thermal reaction (b) oxidized diamond supported catalyst (Sb_2O_4 3%/O-Dia). Catalyst = 100 mg, reaction temperature = 573–873 K, SV = 18,000 mL h^{-1} g-cat^{-1}, gas flow = 30 mL/min (CH_3CHO(0.95%-N_2 balance)/O_2/Ar = 3/5/22). (●) CH_3CHO conversion, (◯) HCHO selectivity, (□) CO_x selectivity.

On the supports other than O-Dia, very small amounts of oxygenates were obtained (runs 15–18). Again, Al_2O_3 and MgO supported catalysts showed high ethane conversion with large amounts of CO_x, indicating that complete oxidation of ethane proceeded on these catalysts (runs 17, 18)

$$C_2H_6 + 7/2O_2 \rightarrow 2CO_2 + 3H_2O, \quad \Delta H^{\circ}_{298} = -1560\,\text{kJ/mol} \tag{11}$$

3.4. Effect of antimonic acid-loading level on the selective oxidation of methane to formaldehyde

Table 4 summarizes the effect of the antimonic acid-loading level on the methane conversion, product yields and selectivities. As described below, after calcianation of the as-prepared catalyst, antimonic acid on O-Dia was transformed into Sb_2O_4. With an increase in the loading level of Sb_2O_4, selective oxidation proceeded and the yield of formaldehyde showed the maximum at 3.0 wt.% (run 22). The CO and CO_2 yields decreased with an increase in the loading level. On the bare O-Dia support without antimony oxide or catalysts with low loading of antimony oxide, a large amount of CO_2 was produced (runs 19, 20). One possible reason for this seems to be combustion of O-Dia support.

Fig. 2 shows TPO patterns of O-Dia and Sb_2O_4 loaded O-Dia at different loading levels. Bare O-Dia was be oxidized at 773 K

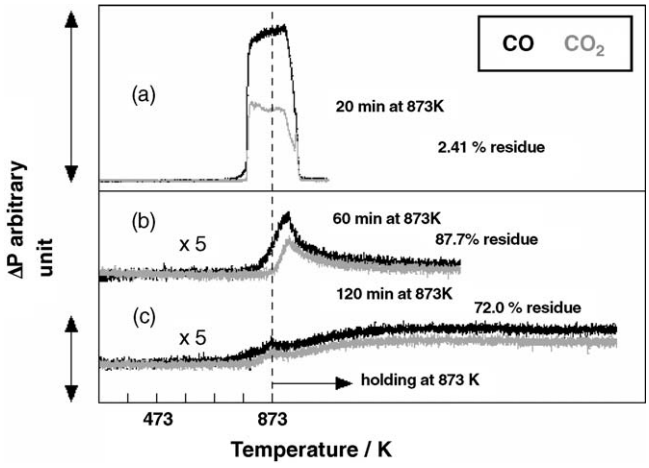

Fig. 2. TPO patterns of Sb_2O_4 loaded O-Dia sample: 100 mg, Ar: 25 mL/min, O_2: 5 mL/min, heting rate: 10 K/min to 873 K, holding time at 873 K: 20 min. (a) O-Dia, (b) Sb_2O_4 (3 wt.%)/O-Dia, (c) Sb_2O_4 (7 wt.%)/O-Dia.

Table 4
Effect of loading level of Sb2O4 on the selective oxidation of methane

Run	Loading level (wt.%)	Conv. (%)	Yield (mmol h^{-1} g-cat^{-1})			Selectivity (%)		
			HCHO	CO	CO_2	HCHO	CO	CO_2
19	0.0	–	0.00	0.11	48.00	0.0	0.2	99.8
20	1.0	–	0.33	0.98	22.70	1.4	4.3	94.5
21	2.0	1.31	0.82	3.06	4.56	9.6	36.3	54.1
22	3.0	0.88	1.32	2.59	1.61	23.9	47.0	29.2
23	3.3	0.66	1.10	1.79	1.10	27.5	45.0	27.5
24	7.0	0.63	1.02	1.67	1.17	26.3	43.3	30.4
25	10.0	0.69	0.93	1.76	1.55	21.9	41.6	36.6

Catalyst: 100 mg, Sb_2O_4 loading level: 3.3 wt.%, reaction temperature: 873 K (0 wt. % at 823 K), gas flow: 30 mL/min (CH_4/O_2 = 25/5), SV: 18,000 mL h^{-1} g-cat^{-1}, reaction time: 90 min.

and while the temperature was kept at 873 K for 20 min, almost all O-Dia was burnt out

$$C\,(\text{diamond}) + O_2 \rightarrow CO_2 \quad (12)$$

As the loading level of antimony oxide increased, the amount of CO and CO_2 formed decreased; this may be corresponding to the fact that antimony oxide is used as a flame retardant [44]. Therefore, antimony oxides might have a role in protecting the O-Dia surface from combustion. Oxidation of O-Dia above 500 °C markedly decreased with loading of Sb_2O_4 (3–7 wt.%) as revealed by TPO in O_2 and Ar mixed gas (Fig. 2b, c).

In order to improve catalytic activity and selectivity, binary systems of Sb_2O_4 combined with V_2O_5, Bi_2O_3 or MoO_3 were examined. However, all these additives did not promote selective oxidation but decreased methane conversion.

3.5. Effect of reaction temperature on the selective oxidation of methane to formaldehyde

Table 5 shows the effect of the reaction temperature on the selective oxidation of methane over the O-Dia supported catalyst. Below 773 K, the reaction did not proceed and the selective oxidation of methane to formaldehyde occurred at above 823 K (run 26). The yield of formaldehyde markedly increased with increasing reaction temperature, and the highest formaldehyde yield was obtained at 873 K (run 27). The formaldehyde selectivity, however, decreased with increasing reaction temperature, since the consecutive oxidation to CO_x occurred. The antimony oxide began to sublime above the reaction temperature of 873 K. However, at 873 K the yield of HCHO did not change for at least 12 h over the Sb_2O_4 loaded O-Dia catalyst.

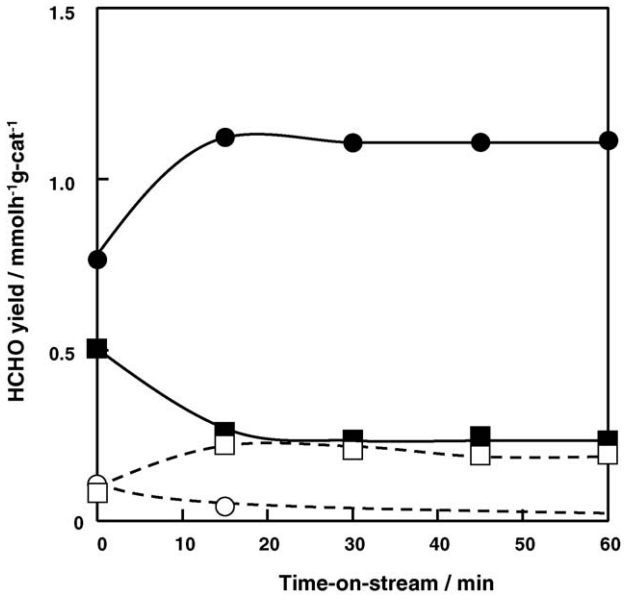

Fig. 3. Time-on-stream of formaldehyde yield in the selective oxidation of methane. Catalyst = 100 mg, Sb_2O_4 loading level = 3 wt.%, reaction temperature = 873 K, gas flow = 30 mL/min (CH_4/O_2 = 25/5), SV = 18,000 mL h^{-1} g-cat^{-1}. (●) Sb oxide/O-Dia, (○) O-Dia, (■) Sb oxide/SiO_2, (□) SiO_2.

3.6. Comparison between antimony oxide-loaded oxidized diamond and SiO_2 catalysts

Fig. 3 shows formaldehyde yield against a time-on-stream in the selective oxidation of methane to formaldehyde over O-Dia and SiO_2 supported catalysts. Here we used a low surface area spherical SiO_2 (SA = 12 m^2/g) in order to compare with O-Dia. Both SiO_2 alone and antimony oxide supported on SiO_2

Table 5
Effect of reaction temperature on the selective oxidation of methane

Run	Reaction temp. (K)	Conv. (%)	Yield (mmol h^{-1} g-cat^{-1})			Selectivity (%)		
			HCHO	CO	CO_2	HCHO	CO	CO_2
26	823	0.20	0.46	0.37	0.43	36.6	29.4	34.0
27	873	0.66	1.10	1.79	1.10	27.5	45.0	27.5
28	923	1.71	1.54	5.16	3.96	14.6	48.3	37.1

Catalyst: 100 mg, Sb_2O_4 loading level: 3.3 wt.%, gas flow: 30 mL/min (CH_4/O_2 = 25/5), SV: 18,000 mL h^{-1} g-cat^{-1}, reaction time: 90 min.

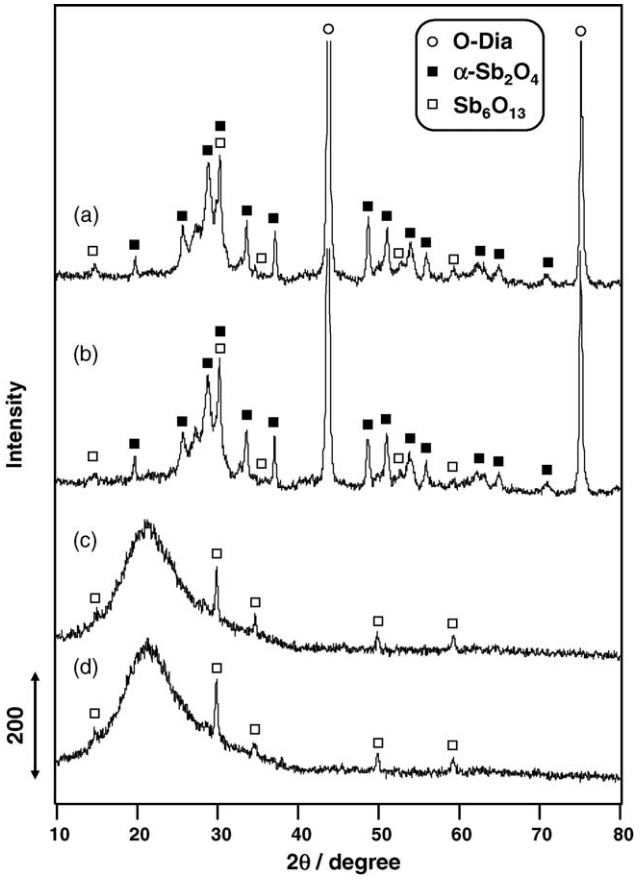

Fig. 4. XRD patterns of Sb_2O_4 loaded catalysts. Loading level 5 wt.%. (a) Fresh Sb_2O_4 loaded O-Dia catalyst calcined at 723 K for 3 h. (b) After reaction of CH_4 with O_2 over (a), (c) fresh Sb_2O_4 loaded SiO_2 catalyst calcined at 773 K for 3 h. (d) After reaction of CH_4 with O_2 over (c).

produced similar amount of formaldehyde. Therefore, antimony oxide on the SiO_2 seems not to have catalytic activity. On the other hand, O-Dia support alone did not produce formaldehyde, and O-Dia supported antimony oxide produced a significant amount of formaldehyde, indicating that only antimony oxide on the O-Dia exhibited catalytic activity.

Zhang et al. obtained considerable yield of HCHO on SiO_2 supported Sb_2O_5 catalyst in the selective oxidation of methane with oxygen [42]. Such differences may partly be ascribed to the differences in the antimony sources. They used chlorides of antimony and we used antimonic acid as a source for impregnation.

Fig. 4 shows the X-ray diffraction (XRD) patterns of O-Dia and SiO_2 supported catalysts before and after the reaction at 873 K. Powdered diamond has no pore structure; therefore all antimony oxide species seems to be dispersed on the diamond surface. O-Dia supported catalyst exhibited strong diffraction peaks of α-Sb_2O_4 and weak diffraction peaks of Sb_6O_{13}. On the other hand, SiO_2 supported catalyst exhibited diffraction peaks of Sb_6O_{13}. Both of the catalysts did not change their diffraction patterns before and after the reaction. Cody et al reported that heating of antimonic acid above 573 K afforded Sb_6O_{13} whereas α-Sb_2O_4 phase appeared above 1000 K [45]. The formation of Sb_6O_{13} on SiO_2 was further confirmed by the IR spectra shown

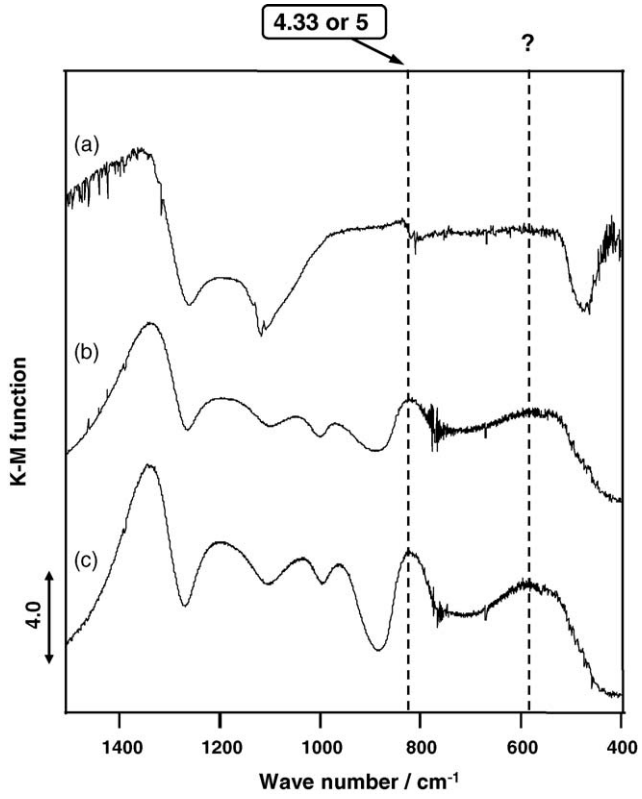

Fig. 5. IR spectra of SbOx loaded SiO_2. (a) SiO_2 (Merck), (b) SbO_x/SiO_2, (c) SbO_x/SiO_2 after the selective oxidation of methane for 2 h at 873 K.

in Fig. 5. In these spectra, a broad absorption band at 820 cm^{-1} ascribed to Sb_6O_{13} (see Fig. 10 trace b) was observed in both fresh and used catalysts (see Fig. 5).

The selective oxidation of methane to formaldehyde over various un-supported antimony oxides was carried out in order to clarify the active species. Results are shown in Fig. 6. Both

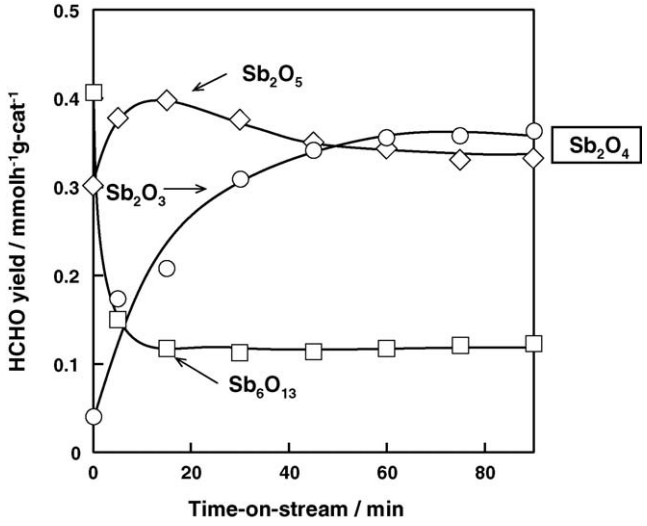

Fig. 6. Time-on-stream of formaldehyde yield in the selective oxidation of methane. Catalyst = 100 mg, unsupported oxides were used, reaction temperature = 873 K, gas flow = 30 mL/min (CH_4/O_2 = 25/5), SV = 18,000 mL h^{-1} g-cat^{-1}. (◯) Sb_2O_3, (□) Sb_6O_{13}, (◊) Sb_2O_5. Sb_2O_4 indicates crystalline form of the catalysts after the reaction.

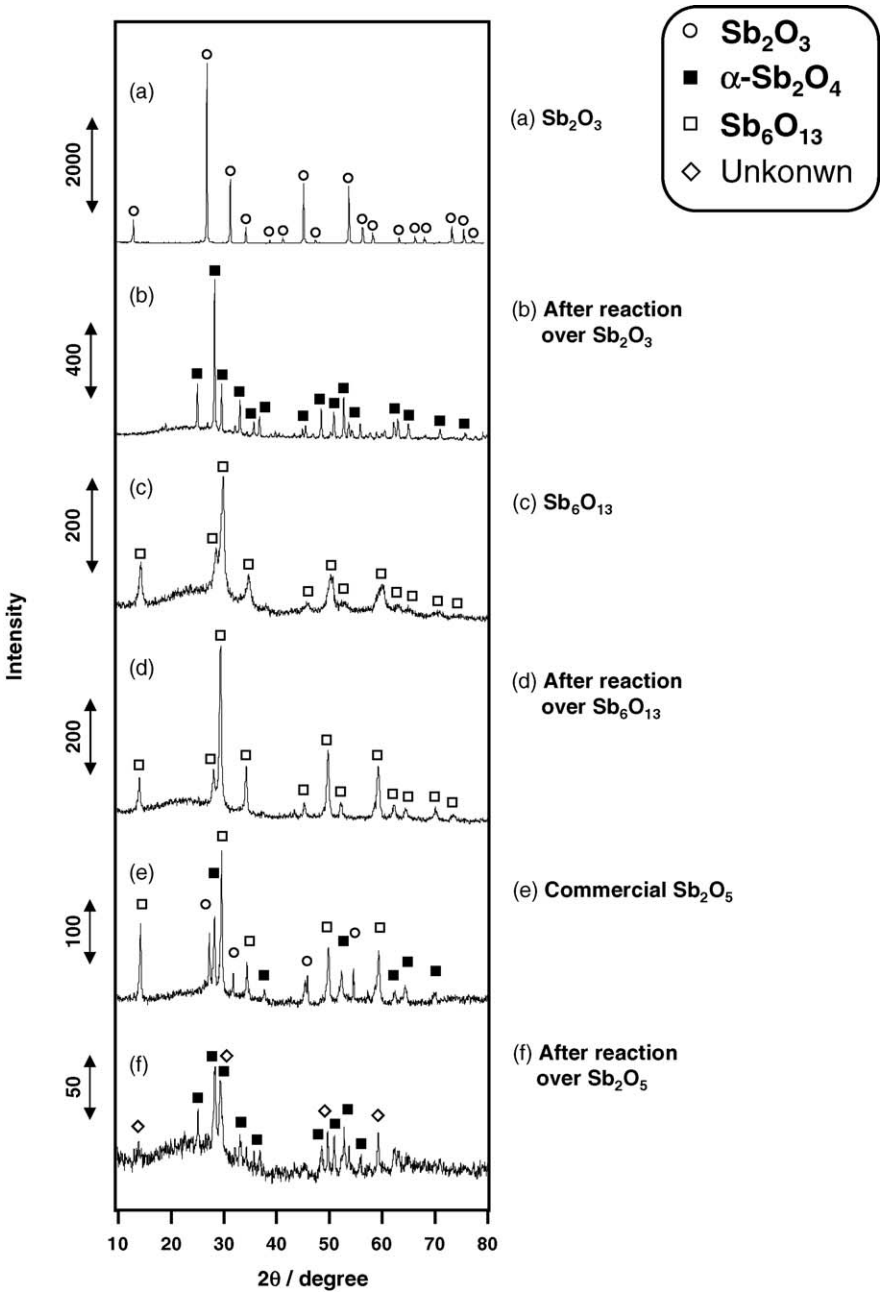

Fig. 7. XRD patterns of unsupported antimony oxides before and after selective oxidation of methane. (a) Sb_2O_3, (b) after reaction over Sb_2O_3, (c)Sb_6O_{13}, (d) after reaction over Sb_6O_{13}, (e) commercial Sb_2O_5, (f) after reaction over Sb_2O_5. Catalyst = 100 mg, reaction temperature = 873 K, gas flow = 30 mL/min (CH_4/O_2 = 25/5), SV = 18,000 mL h^{-1} g-cat^{-1}.

commercial Sb_2O_3 and Sb_2O_5 produced about 0.3 mmol h^{-1} g-cat^{-1} of formaldehyde, and the formaldehyde yield gradually increased in the initial 60 min over Sb_2O_3. On the other hand, the formaldehyde yield on Sb_6O_{13} decreased from 0.4 to 0.1 mmol h^{-1} g-cat^{-1} in the initial 15 min.

Fig. 7 shows the XRD patterns of un-supported antimony oxides before and after the selective oxidation of methane at 873 K. As seen in Fig. 5, Sb_2O_3 was transformed into α-Sb_2O_4 during the reaction. Commercial Sb_2O_5 was identified as a mixture of Sb_6O_{13}, α-Sb_2O_4 and Sb_2O_3. After the reaction, the mixture was predominantly transformed into the α-Sb_2O_4 phase with several unidentified peaks. Powder X-ray diffraction patterns of antimony oxides are variable depending on the morphology of crystal [46]. Commercial Sb_6O_{13} was not transformed into α-Sb_2O_4 and remained in its original form only with growth in the crystallite size (sharper diffraction peaks). These results suggest that the active form of antimony oxide is α-Sb_2O_4. On the other hand, Sb_6O_{13} is stable under the reaction conditions and the selective oxidation proceeded only to a small extent. Therefore, O-Dia could be a good support keeping antimony oxide as Sb_2O_4, while SiO_2 was not a favorable support for keeping antimony oxide as Sb_2O_4.

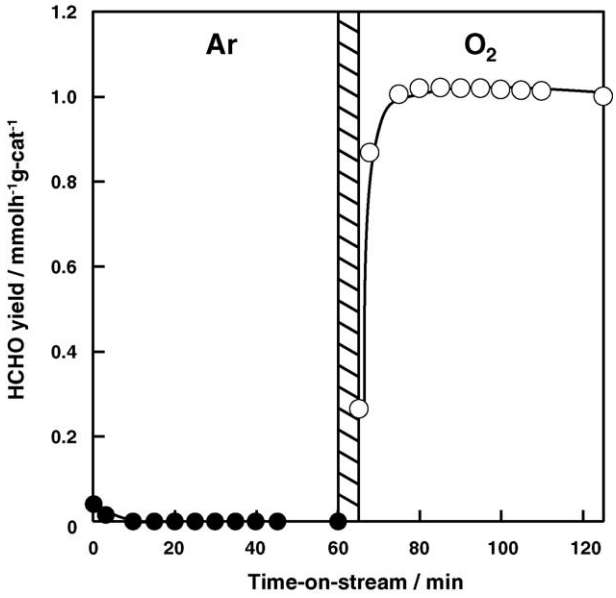

Fig. 8. Influence of atmosphere on formaldehyde yield. Ar and CH_4 flow was switched to O_2 and CH_4 flow after the run for 60 min. Catalyst = 100 mg, Sb_2O_4 (3 wt.%) on O-Dia, reaction temperature = 873 K, gas flow = 30 mL/min (CH_4/Ar or O_2 = 25/5), SV = 18,000 mL h^{-1} g-cat^{-1}.

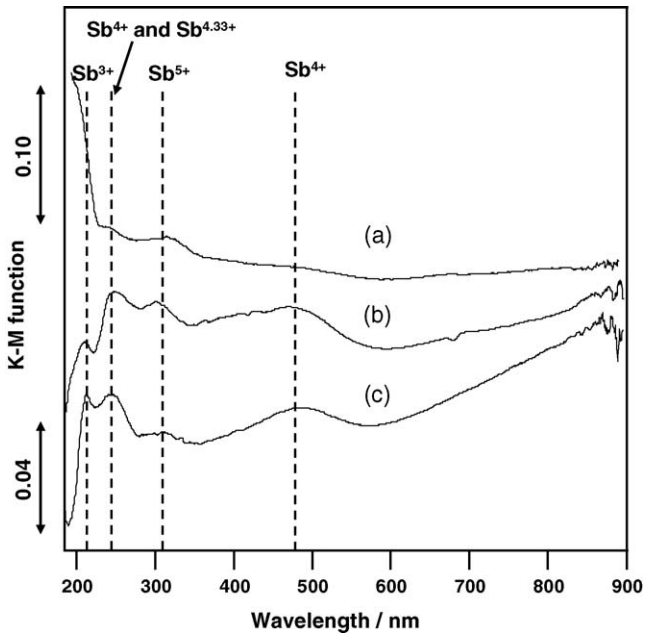

Fig. 9. Diffuse reflectance UV–vis spectra of Sb_2O_4 loaded catalysts. (a) O-Dia, (b) Sb_2O_4/O-Dia, (c) after the selective oxidation of methane on Sb_2O_4/O-Dia in CH_4/O_2 = 25/5. Loading level 3 wt.% Samples was measure by diluting with SiO_2 (sample:SiO_2 = 1:2).

The average turnover frequency (TOF) to formaldehyde during the reaction from 30 to 90 min was calculated as 13.5 mol formaldehyde h^{-1}/mol Sb_2O_4 on O-Dia. Although the number of active centers in the oxide-based catalyst cannot accurately be evaluated, it can be expected that the TOF per active center would be much higher.

3.7. Valence state of antimony oxide on oxidized diamond supported catalyst

Fig. 8 shows the change in the formaldehyde yield by switching Ar atmosphere to O_2 during the reaction over the SbO_x loaded O-Dia catalyst. Under Ar flow, the formation of formaldehyde was observed only in the initial short period, and the yield of formaldehyde rapidly decreased by the consumption of active oxygen in the antimony oxide lattice on the O-Dia surface. When the flowing gas was switched from Ar to O_2, oxygen defect on the antimony oxide on the O-Dia was rapidly recovered and the yield of formaldehyde rapidly increased.

Fig. 9 shows the diffuse reflectance UV–vis spectra of the O-Dia supported catalyst before and after the selective oxidation of methane in O_2. The profile of fresh catalyst contained various antimony oxides that are assigned to Sb^{3+} (195–230 nm), Sb^{4+} and $Sb^{4.33+}$ (230–280 nm and 480 nm) and Sb^{5+} (300–340 nm). Although these values are not consistent with those reported in the literature [47], XRD data of these samples support our present UV–vis assignments. After the selective oxidation of methane with O_2 at 873 K, the absorption assigned to Sb^{3+} species increased. This indicates that slight loss of surface oxygen from Sb_2O_4 proceeded during the oxidation.

X-ray photoelectron spectra revealed the same features as observed with UV–vis spectra, where the fresh Sb_2O_4/O-Dia catalyst exhibited a broad peak at 543.2 eV (Sb $3d_{3/2}$). After the reaction, an overlapping peak appeared at 541.0 eV (Sb_2O_3 Sb $3d_{3/2}$).

IR spectra of SbO_x loaded on O-Dia are shown in Fig. 10. In the IR absorption, broad bands at 780–690 cm^{-1} on α-Sb_2O_4/O-

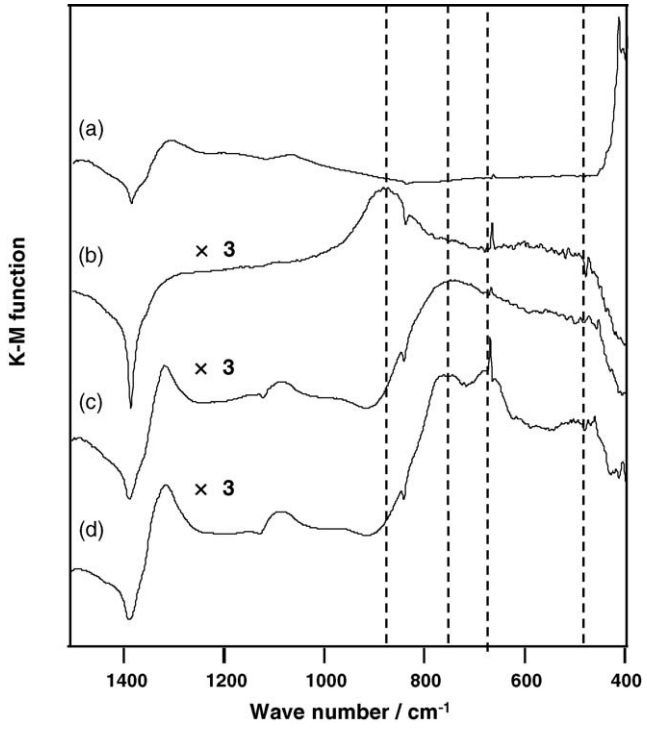

Fig. 10. Diffuse reflectance IR spectra of Sb_2O_4/O-Dia before and after the selective oxidation of methane. (a) O-Dia, (b) Sb_6O_{13} bulk sample, (c) fresh catalyst after calcinations at 723 K for 3 h, (d) after the selective oxidation of methane at 873 K for 1.5 h.

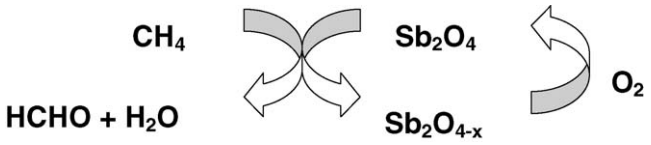

Scheme 1. Catalytic cycle of selective oxidation.

Dia catalyst were observed throughout the reaction, indicating that Sb_2O_4 was the predominant phase on O-Dia [45]. During the selective oxidation, peaks at 780, 690 and 480 cm^{-1} increased. Slight increase in peaks around 1100 cm^{-1} was seen and this seems to be ascribed to the Sb^{3+} species. Increase in the absorption at 480 cm^{-1} could not be interpreted at present.

These results seem to indicate that a certain portion of lattice oxygen of α-Sb_2O_4 on the O-Dia was consumed in reacting with methane leaving Sb_2O_{4-x}. The reduced Sb_2O_{4-x} on the O-Dia could be re-oxidized to α-Sb_2O_4 by O_2 in the gas phase. Therefore, it is strongly suggested that the redox cycle existed between α-Sb_2O_4 and Sb_2O_{4-x} (Scheme 1).

4. Conclusions

Antimony oxide supported on the oxidized diamond showed a moderate catalytic activity for the selective oxidation of methane to formaldehyde. It was suggested that the reaction proceeded by a redox mechanism between Sb_2O_4 and Sb_2O_{4-x}, while stable Sb_6O_{13} was almost inactive.

Acknowledgment

This work was partly supported "Hi-Tech Research Center" Project for Private Universities: by matching fund subsidy from Ministry of Education, Culture, Sports, Science and Technology (2003-2007).

References

[1] A. Parmaliana, F. Arena, J. Catal. 167 (1997) 57–65.
[2] F. Arena, N. Giordano, A. Parmaliana, J. Catal. 167 (1997) 66–76.
[3] H.-F. Lin, R.-S. Liu, K.Y. Liew, R.E. Johnson, J.H. Lunsford, J. Am. Chem. Soc. 106 (1984) 4117–4121.
[4] N.D. Spencer, J. Catal. 109 (1988) 187–197.
[5] T. Suzuki, K. Wada, M. Shima, Y. Watanabe, J. Chem. Soc., Chem. Commun. (1990) 1159–1160.
[6] L.-X. Dai, Y.-H. Teng, K. Tabata, E. Suzuki, T. Tatsumi, Chem. Lett. 29 (2000) 794–795.
[7] A. de Lucas, J.L. Valverde, L. Rodriguez, P. Sanchez, M.T. Garcia, Appl. Catal. A 203 (2000) 81–90.
[8] X. Zhang, D.-H. He, Q.-J. Zhang, Q. Ye, B.-Q. Xu, Q.-M. Zhu, Appl. Catal. A 249 (2003) 107–117.
[9] Y. Wang, K. Otsuka, J. Chem. Soc., Chem. Commun. (1994) 2209–2210.
[10] A. Parmaliana, F. Arena, F. Frusteri, A. Martinez-Arias, M.L. Granados, J.L.G. Fierro, Appl. Catal. A 226 (2002) 163–174.
[11] M.M. Koranne, J.G. Goodwin Jr., G. Marcelin, J. Catal. 148 (1994) 378–387.
[12] C.-B. Wang, R.G. Herman, C. Shi, Q. Sun, J.E. Roberts, Appl. Catal. A 247 (2003) 321–333.
[13] V. Fornes, C. Lopez, H.H. Lopez, A. Martinez, Appl. Catal. A 249 (2003) 345–354.
[14] B. Lin, X. Wang, Q. Guo, W. Yang, Q. Zhang, Y. Wang, Chem. Lett. 32 (2003) 860–861.
[15] H. Berndt, A. Martin, A. Brückner, E. Schreier, M. Müller, H. Kosslick, G.-U. Wolf, B. Lücke, J. Catal. 191 (2000) 384–400.
[16] Q. Zhang, W. Yang, X. Wang, Y. Wang, T. Shishido, K. Takehira, Micropor. Mesopor. Mater. 77 (2005) 223–234.
[17] Y. Teng, F. Ouyang, L. Dai, T. Karasuda, H. Sakurai, K. Tabata, E. Suzuki, Chem. Lett. 28 (1999) 991–992.
[18] T. Takemoto, K. Tabata, Y. Teng, A. Nakayama, E. Suzuki, Appl. Catal. A 205 (2001) 51–59.
[19] K. Tabata, Y. Teng, T. Takemoto, E. Suzuki, M.A. Banares, M.A. Pena, J.L.G. Fierro, Catal. Rev. 44 (2002) 1–58.
[20] C. Batiot, B.K. Hodnett, Appl. Catal. A 137 (1996) 179–191.
[21] K. Nakagawa, C. Kajita, N. Ikenaga, T. Kobayashi, M.N. -Gamo, T. Ando, T. Suzuki, Chem. Lett. 29 (2000) 1100–1101.
[22] H. Nishimoto, K. Nakagawa, N. Ikenaga, M.N. -Gamo, T. Ando, T. Suzuki, Appl. Catal. A 264 (2004) 65–72.
[23] K. Nakagawa, K. Okumura, T. Shimamura, N. Ikenaga, T. Suzuki, T. Kobayashi, M.N. -Gamo, T. Ando, Chem. Lett. 32 (2003) 866–867.
[24] K. Okumura, K. Nakagawa, T. Shimamura, N. Ikenaga, M.N. -Gamo, T. Ando, T. Kobayashi, T. Suzuki, J. Phys. Chem. B 107 (2003) 13419–13424.
[25] T. Shimamura, K. Okumura, K. Nakagawa, T. Ando, N. Ikenaga, T. Suzuki, J. Mol. Catal. A 211 (2004) 97–102.
[26] M.D. Allen, S. Poulston, E.G. Bithell, M.J. Goringe, M. Bowker, J. Catal. 163 (1996) 204–214.
[27] G. Centi, P. Mazzoli, S. Perathoner, Appl. Catal. A 165 (1997) 273–290.
[28] M.O. Guerrero-Perez, M.A. Banares, Chem. Commn. (2002) 1292–1293.
[29] G. Centi, F. Guarnieri, S. Perathoner, J. Chem. Soc., Faraday Trans. 93 (1997) 3391–3402.
[30] A. Wickman, L.R. Wallenberg, A. Andersson, J. Catal. 194 (2000) 153–166.
[31] N. Ballarini, F. Cavani, M. Cimini, T. Trifiro, R. Catani, U. Cornaro, D. Ghisletti, Appl. Catal. A 251 (2003) 49–59.
[32] J. Nilsson, A.R. Landa-Canovas, S. Hansen, A. Andersson, J. Catal. 186 (1999) 442–457.
[33] L.C. Brazdil, A.M. Ebner, J.F. Brazdil, J. Catal. 163 (1996) 117–121.
[34] J. Nilsson, A.R. Landa-Canovas, S. Hansen, A. Andersson, J. Catal. 160 (1996) 244–260.
[35] H.W. Zanthoff, S. Schaefer, G.-U. Wolf, Appl. Catal. A 164 (1997) 105–117.
[36] G. Centi, F. Marchi, S. Perathoner, Appl. Catal. A 149 (1997) 225–244.
[37] Y.A. Saleh-Alhamed, R.R. Hudgins, P.L. Silveston, J. Catal. 161 (1996) 430–440.
[38] F.J. Berry, Adv. Catal. 30 (1981) 97–131.
[39] E.V. Steen, M. Schnobel, R. Walsh, T. Riedel, Appl. Catal. A 165 (1997) 349–356.
[40] P. Botella, P. Concepcion, J.M.L. Nieto, B. Solsona, Catal. Lett. 89 (2003) 249–253.
[41] W. Ueda, K. Oshihara, Appl. Catal. A 200 (2000) 135–143.
[42] H. Zhang, P. Ying, J. Zhang, C. Liang, Z. Feng, C. Li, Stud. Surf. Sci. Catal. 147 (2004) 547–552.
[43] T. Ando, K. Yamamoto, M. Ishii, M. Kamo, Y. Sato, J. Chem. Soc. Faraday Trans. 89 (1993) 3635–3640.
[44] C.P. Fenimore, F.J. Martin, Combust. Flame 10 (1966) 135–139.
[45] C.A. Cody, L. Dicarlo, R.K. Darlington, Inorg. Chem. 18 (1979) 1572–1576.
[46] K.A.L. Abdelouabad, U. Roullet, M. Brun, A. Burrows, C.J. Kiely, J.C. Volta, M. Abon, Appl. Catal. A 210 (2001) 12–136.
[47] F. Sala, F. Trifro, J. Catal. 34 (1974) 68–78.